Analytica Chimica Acta 1206 (2022) 339761

Contents lists available at ScienceDirect

Analytica Chimica Acta

journal homepage: www.elsevier.com/locate/aca

Single cell mass spectrometry studies reveal metabolomic features and potential mechanisms of drug-resistant cancer cell lines

Mei Sun [a, 2, 1], Xingxiu Chen [a, 1], Zhibo Yang [a, *]

[a] Department of Chemistry and Biochemistry, University of Oklahoma, Norman, OK, 73019, USA

HIGHLIGHTS

- Live single cell mass spectrometry was combined with other bio-analytical techniques.
- Cells' molecular profiles were correlated to their resistance to anticancer drug.
- Metabolomic biomarkers and relevant proteins reflecting cancer cells' drug resistance were proposed.
- Drug resistant cancer cells possess molecular features similar to cancer stem cells.

GRAPHICAL ABSTRACT

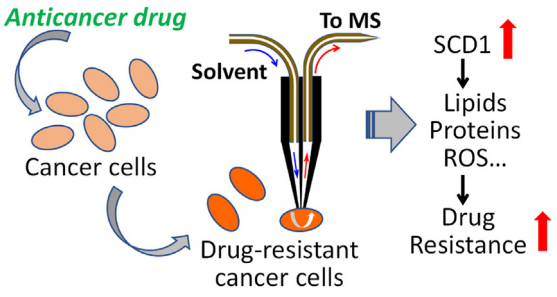

ARTICLE INFO

Article history:
Received 5 December 2021
Received in revised form
18 March 2022
Accepted 22 March 2022

ABSTRACT

Irinotecan (Iri) is a key drug to treat metastatic colorectal cancer, but its clinical activity is often limited by *de novo* and acquired drug resistance. Studying the underlying mechanisms of drug resistance is necessary for developing novel therapeutic strategies. In this study, we used both regular and irinotecan-resistant (Iri-resistant) colorectal cell lines as models, and performed single cell mass spectrometry (SCMS) metabolomics studies combined with analyses from cytotoxicity assay, western blot, flow cytometry, quantitative real-time polymerase chain reaction (qPCR), and reactive oxygen species (ROS). Our SCMS results indicate that Iri-resistant cancer cells possess higher levels of unsaturated lipids compared with the regular cancer cells. In addition, multiple protein biomarkers and their corresponding mRNAs of colon cancer stem cells are overexpressed in Iri-resistance cells. Particularly, stearoyl-CoA desaturase 1 (SCD1) is upregulated with the development of drug resistance in Iri-resistant cells, whereas inhibiting the activity of SCD1 efficiently increase their sensitivity to Iri treatment. In addition, we demonstrated that SCD1 directly regulates the expression of ALDH1A1, which contributes to the cancer stemness and ROS level in Iri-resistant cell lines.

1. Introduction

Cancer is a devastating disease in the world [1], and chemotherapy is one of the major treatment options for cancer [2]. Chemotherapy utilizes drug compounds to treat cancers at different stages, and it can also be used as an adjuvant therapy after surgery [3]. Unfortunately, cancer cell subpopulations possessing drug resistance, including intrinsic resistance and acquired

* Corresponding author. Department of Chemistry and Biochemistry, University of Oklahoma, Norman, OK, 73019, USA.
E-mail address: zhibo.yang@ou.edu (Z. Yang).
[2] Current addresses: PTC Therapeutics, Inc., South Plainfield, NJ 07080.
[1] Mei Sun and Xingxiu Chen contributed equally to this work.

https://doi.org/10.1016/j.aca.2022.339761
0003-2670/

resistance, can survive from chemotherapy and greatly reduce the therapeutic efficiency, eventually resulting in the chemotherapy failure [4]. Thus, understanding the drug resistant mechanisms of rare cancer cells is critical for both fundamental cancer research and the development of more effective therapeutics.

Previous studies revealed a number of drug resistant mechanisms, including enhanced drug efflux, increased drug inactivation, promoted DNA damage repair, and suppressed apoptosis pathway, in cancers [4,5]. Accumulating evidence indicates that the development of drug resistance is associated with alterations of metabolic profiles. For example, glycolytic pyruvate can regulate the expression of P-glycoprotein, a drug efflux pump, in multicellular tumor spheroids, and the level of pyruvate in cells is correlated to intracellular drug abundance [6–8]. Moreover, the activity of ATP-binding cassette transporters are directly related to ATP level, and increasing the level of ATP will promote drug efflux and drug chemoresistance [9]. Therefore, studying metabolic alterations in drug resistant cancer cells can improve our understanding of drug resistance mechanisms and provide potential molecular targets to treat drug resistant cancer cell.

Cancer cells with acquired drug resistant are normally generated through repeated treatment using clinically relevant drug compounds [10,11]. In most studies, cancer cells are treated with gradually increased dose of anticancer drugs for an extended period of time (e.g., 6–12 months or longer) to develop the drug-resistant cell models [12]. In contrast, only a very few studies have been conducted using cells possessing early-stage drug resistance to investigate their metabolic features and biological changes. In fact, initial drug resistance is strongly related to chemotherapy treatment failure, and additional treatment, such as second-line drug, is recommended to improve the efficacy of chemotherapy during early-stage of drug treatment [13,14]. Understanding the metabolic alternation involved in the beginning of drug resistance development can reveal the relevant mechanisms and eventually benefit the disease management.

In addition to the metabolic changes, chemotherapy can lead to the enrichment of the CSCs, which are small sub-populations of stem-like cancer cells with self-renew and spheroid formation characteristics [15]. CSCs can be isolated from various types of tumors, and they possess high levels of resistance to numerous anticancer drugs, such as oxaliplatin and 5-fluorouracil [16], promoting tumor recurrence and metastasis [17,18]. However, the specific mechanisms of drug-induced cancer stemness still remain unclear, limiting the efficacy of clinical thermotherapy [19,20].

Due to its high detection sensitivity, broad range of molecular coverage, and rich structure information, mass spectrometry (MS) has become a powerful tool for metabolomics studies of biological samples such as tissues and cells. In conventional metabolomics studies, samples are converted into lysates containing molecules from populations of cells, and then analyzed using traditional liquid chromatography–MS (LC-MS) platforms. However, due to cell heterogeneity and limited quantity of rare types of cells, particularly those from patients in clinical treatment, it is impractical to perform molecular analysis using these traditional analytical methods. In addition, cell metabolites are directly related to cellular processes, and their compositions are rapidly altered by cell environment [21,22]. The obligatory sample preparation prior to traditional analysis will inevitably change cell metabolism and molecular composition. For example, compared with LC-MS results, our previous studies indicate certain cell metabolites can be only detected from SCMS analyses of live cells [23]. In quantitative studies of drug uptake, obligatory sample preparation in traditional LC/MS experiments can potentially induce loss of drug molecules from cells [24]. Therefore, techniques allowing for analysis of individual live single cells, such as ambient single-cell mass spectrometry (SCMS) methods, would provide a great advantage to effectively study subpopulation cells, including those possessing drug resistance, among heterogeneous cells. A variety of different SCMS techniques have been developed to date. Secondary ion MS (SIMS) and matrix-assisted laser desorption ionization MS (MALDI-MS) are two typical methods requiring vacuum environment for molecular sampling and ionization, indicating these methods are not suitable to analyze live cells [25,26]. To overcome these inherent drawbacks, ambient-based techniques, including live single-cell MS [27], probe ESI MS [28], laser ablation electrospray ionization (LAESI) [29], capillary microsampling ESI-IMS-MS [22], have been developed to perform analyses of live cells in ambient environment. Our group has established multiple ambient SCMS methods, including the Single-probe [30,31], T-probe [32,33], and micropipette [34]. Among them, the Single-probe is a multifunctional device capable of sampling and ionizing contents in live single cells for real-time MS measurements. The Single-probe SCMS technique has been used to analyze intracellular metabolites [23,31,35–39] and quantify the amount of drug uptake using cell lines [24,40,41] and patient cells [42]. In addition, this device has been utilized for high-resolution MS imaging of biological tissue slices [31,43–46] and analysis of extracellular metabolites in live multicellular spheroids [47].

In this study, we applied the Single-probe SCMS technique to explore the metabolic differences between the parental HCT-116 colorectal cancer cells and the corresponding drug-resistant cells at the single-cell level in ambient environment. Combined with other analytical techniques (e.g., cytotoxicity assay, western blot analysis, flow cytometry, and quantitative real-time polymerase chain reaction (qPCR)), we investigated the molecular mechanisms of cancer cells possessing early-stage of resistance to irinotecan (Iri), a widely used antitumor drug. We observed that Iri-resistant cells acquired certain molecular characteristics related to cancer stemness, and we discovered a new drug-resistance mechanism: Iri-resistant cells upregulate the expression of stearoyl-CoA desaturase-1 (SCD1) and increase reactive oxygen species (ROS) level. This study can establish an approach to understanding of early-stage development of drug-resistance of cancer cells, and potentially benefit early diagnosis of patients with drug-resistance and the development of novel therapeutic strategies.

2. Methods

2.1. Cell lines and cell culture

HCT-116 cells were originally obtained from American Type Culture Collection (ATCC) (Rockville, MD, USA). Cells were cultured in McCoy's 5A cell culture medium (Life Technologies, Grand Island, NY, USA) containing 10% FBS (fetal bovine serum; Life Technologies, Grand Island, NY, USA) and 1% Pen Strep (Life Technologies, Grand Island, NY, USA) at 37 °C in an incubator with 5% CO_2 supply (HeraCell, Heraeus, Germany). The stock solution of Iri was prepared in dimethyl sulfoxide (DMSO; Sigma-Aldrich, St. Louis, MO, USA). In order to obtain Iri-resistant cells, parental HCT-116 cells were incubated in medium containing 1.0 μM of Iri (Life Technologies, Grand Island, NY, USA). Survived cells were then passaged at 80% confluence for incubation at 1.0 μM of Iri. To establish Iri-resistant cells with different resistance levels, these processes were repeated for 3, 10, and 20 days to obtain 3-, 10-, and 20-day resistant cells, respectively.

2.2. Cytotoxicity assay

The MTT ((3-(4,5-Dimethylthiazol-2-yl)-2,5-Diphenyltetrazolium Bromide) (BIOTIUM Inc., Hayward, CA, CA, USA) was used to

determine the growth inhibitory effect of Iri on cell viabilities. IC_{50} (at 72 h) measurements of cells were performed by following the manufacturer's protocols and reported studies [48]. Briefly, cells were seeded into 96-well plate (~10,000 cells per well), and Iri treatment was conducted using a series of concentrations (i.e., 0.1, 1.0, 5.0, 10, and 50 μM) for 72 h. MTT solution was added into each well, followed by incubation (4 h) and addition of DMSO. The absorbance signal at 570 nm was then measured using a microplate reader (Synergy H1, BioTek, Winooski, VE). IC_{50} values were calculated using Prism (GraphPad Software, San Diego, CA, USA).

2.3. The single-probe SCMS experiments

The Single-probe is a microscale sampling and ionization device that can be coupled to mass spectrometer for single cell studies [24,35,47,49–51] and MS imaging of tissues in ambient conditions [43,45,46,52]. The fabrication protocols of the Single-probe have been described in previous studies [50,51]. Briefly, there are three components in a Single-probe: a needle pulled from dual-bore quartz tubing (outer diameter (OD): 500 μm; inner diameter (ID): 127 μm, Friedrich & Dimmock, Inc., Millville, NJ, USA) using a laser pipet puller (P-2000 micropipette puller, Sutter Instrument, Novato, CA, USA), a fused silica capillary (OD: 105 μm; ID: 40 μm, Polymicro Technologies, Phoenix, AZ, USA), and a nano-ESI emitter produced using the same type of fused silica capillary. A Single-probe is fabricated by embedding a laser-pulled dual-bore quartz needle with a fused silica capillary and a nano-ESI emitter (Fig. 1A-B).

During the SCMS experiments, cells were attached on the glass coverslips through over-night culture. Coverslips containing cells were rinsed using fresh culture medium, and placed onto a motorized XYZ−translation stage system, which was controlled using a LabView software package [53], of the Single-probe SCMS setup (Fig. 1b) [51]. A syringe (250 μl; Hamilton Co., Reno, NV, USA) was used to continuously deliver (flow rate: 0.10 μL/min) the sampling solvent (acetonitrile containing 0.1% acetic acid). Once the ionization voltage (applied on the conductive union) was tuned on, a stable liquid junction was formed at the Single-probe tip to extract cellular contents (Fig. 1B). Using the microscope as a visual guide, the tip of the Single-probe (OD ~10 μm) was precisely inserted into a targeted cell. Cellular contents were drawn to the nano-ESI emitter through the capillary action, and immediately ionized for MS analysis using a Thermo LTQ Orbitrap XL mass spectrometer (Thermo Scientific, Waltham, MA, USA). Cellular contents extraction and MS data acquisition were continuously performed till ion signals of cellular contents completely disappeared. Mass analysis parameters are listed as follows: mass range (*m/z*), 200−1500; mass resolution, 60,000; ionization voltage at the positive ion mode, +4.5 kV; microscan, 1; max injection time, 100 ms; AGC (automatic gain control) on.

2.4. Data analysis

Analyses of SCMS data were carried out according to our published protocols [54]. First, we conducted data pretreatment. The raw SCMS data were exported as tab-delimited data files (*m/z* values with their normalized intensities) using Thermo Xcalibur Qual Browser (Thermo Scientific, Waltham, MA, USA). Only relatively abundant peaks (intensity in raw mass spectra > 10^3) were exported, whereas background signals, such as peaks from solvent and cell culture medium, were subtracted from MS data using R script. To minimize the influence induced by fluctuations of ion signals during experiments, ion intensities were normalized to the total ion current (TIC) for following data analysis. Peak alignment was performed using Geena 2 [55]. The normalized intensities of each ion were used to represent its relative abundances in different cells. Second, we performed statistical data analyses using MetaboAnalyst 5.0 [56]. PCA (principal component analysis), an unsupervised multivariate analysis method, was used to compare the overall profiles of metabolites of cells in different groups. Levene's test indicated that our SCMS data have equal variances, and Student's t-test was applied to obtain ions of interest, i.e., ions with significantly different abundance between two groups ($p < 0.05$). In addition, volcano plots were constructed to combine the information of statistical significance (p value) and magnitude of change (fold change) for all species. Third, putative labeling on metabolites of interest was searched in METLIN [57] and HMDB [58] (mass accurate <5 ppm), whereas species of interest were identified by comparing measured MS/MS spectra with online databases (METLIN, HMDB and GNPS [59]) and through manual structure elucidation.

2.5. HPLC-MS/MS

Due to the limited amounts of analytes from single cells, MS/MS measurements can be only conducted for relatively abundant ions. To overcome this challenge, HPLC-MS/MS was used as a complementary method to determine ions of interest, which were determined from the SCMS studies, using cell lysates. Briefly, cell lysates were prepared using the Folch method [60,61]. Cells (~1×10^6) were detached from the petri dish and resuspended into 1 mL PBS (phosphate-buffered saline). 3 mL chloroform/methanol mixture (2:1, v/v) was added into the cell suspension, followed by vertexing (on ice, 10 min) and centrifuge (10 min). The organic layer was dried (SPD111V SpeedVac concentrator, Thermo Scientific, San Jose, CA) for storage (in −80 °C refrigerator). Samples were reconstitution (in

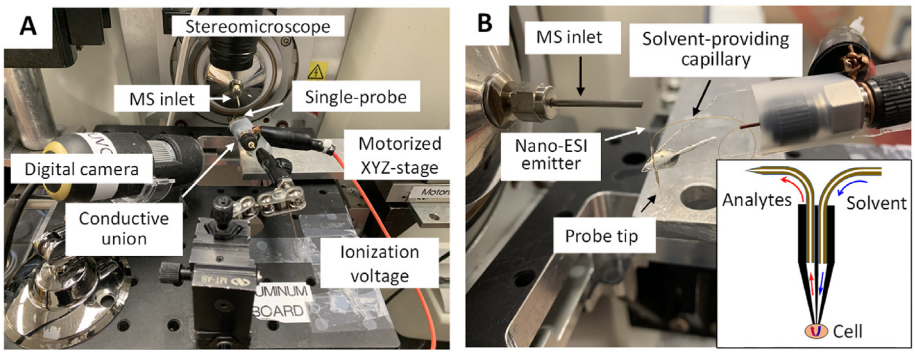

Fig. 1. (A) The single-probe SCMS experimental setup. (B) Zoomed-in photo of the Single-probe coupling with a Thermo LTQ Orbitrap XL mass spectrometer. The schematic drawing and working mechanisms of the Single-probe are illustrated in the inset.

150 μL chloroform) prior to HPLC-MS/MS analysis.

LC-MS/MS analyses were used to provide complementary information for structure identification. Both targeted (i.e., ions of interest from SCMS results) and untargeted analyses were performed. An UltiMate 3000 HPLC system (Thermo Scientific, San Jose, CA) was coupled to the LTQ Orbitrap XL mass spectrometer. A Luca 3u C18 column (50 × 2.00 mm, 3 μm, Phenomenex, Torrance, CA) was used in the LC system. Settings of the LC system include injection volume (2 μL), column temperature (50 °C), mobile phase A (water/methanol (95/5, v/v)), mobile phase B (isopropanol/methanol/water (60/35/5, v/v)), and total run time (80 min). In targeted analysis, the first run (full scan mode) was used to determine the retention time of ions of interest in, and CID (with the normalized collision energy (NCE) as 24–25 (manufactory's unit)) was carried out for MS/MS analyses of targeted ions in the second run. In data dependent mode for untargeted analysis, the same LC settings were used, and MS/MS measurements were performed for the top-five most abundant peaks. The obtained LC-MS data were converted to.mzML format using MSConvertGUI [62], then the MS features were extracted using MZMine 2 in an untargeted manner [63].

2.6. Western blot analysis

Cell lysates (1×10^7 cells for each sample) were prepared using radioimmunoprecipitation assay (RIPA) buffer containing protease inhibitor (Thermo Scientific). Samples containing an equal amount (20 μL, ~20 μg) of proteins were separated using 12% sodium dodecyl sulfate-polyacrylamide gel electrophoresis (SDS-PAGE), and proteins were then transferred to nitrocellulose membranes (GE, Healthcare Life Science, Marlborough, MA, USA). Membranes were blocked by 10% non-fat milk (Bio-Rad Laboratories, Hercules, CA, USA) and incubated overnight with primary antibody at 4°C. Two primary antibodies, anti-SCD1 antibody (Thermo Fisher Scientific, Waltham, MA, USA) and anti-tubulin antibody (Abcam, Cambridge, MA, USA), were used in Western blot analysis. The corresponding secondary antibody, goat anti rabbit IgG (Thermo Fisher Scientific), was added during the incubation (1 h, at room temperature), and then membranes were washed using PBS for three times. Finally, protein bands were vitalized using the Opti-4CN western blot detection kit (Bio-Rad Laboratories).

2.7. Flow cytometry analysis

A Stratedigm S1400Exi flow cytometer (Stratedigm, San Jose, CA, USA) was used to determine the expression of cancer stem cell biomarkers, CD133 and CD24, in Iri-resistant and parental (control) cells. Briefly, cells were suspended in the solution containing 0.5% BSA (bovine serum albumin; Sigma-Aldrich, St. Louis, USA) and antibodies (human anti-CD24-FITC and human anti-CD133-PE; Miltenyi Biotec, Bergisch Gladbach, Germany) on ice. CD133 and CD24 double-positive cells ($CD133^+/CD24^+$) were gated using control cells that incubated with IgG1 isotype control FITC-conjugated antibody and PE-conjugated antibody (Biolegend, San Diego, CA).

2.8. Reactive oxygen species (ROS) measurement

Measurements of reactive oxygen species (ROS) were conducted based on the published protocols [64]. Briefly, cells were incubated in McCoy's 5A cell culture medium containing 1 μM CM-H2DCFDA (cellular ROS indicator; Thermo Fisher Scientific) at 37°C for 30 min, washed using PBS, and then analyzed using a Stratedigm S1400Exi flow cytometer platform.

2.9. RNA extraction and quantitative real-time polymerase chain reaction (qPCR)

The RNeasy Mini Kit (Qiagen Inc, Valencia, CA) was used to isolate RNA from cells according to the manufacturer's instructions. The potential genomic DNA contaminants were removed using a DNA-free™ DNA Removal Kit (Thermo Fisher Scientific). iScript™ Reverse Transcription Supermix (Bio-Rad Laboratories) was used to synthesize the cDNA, and then qPCR experiments were performed using a CFX96 Touch™ Real-Time PCR Detection System (Bio-Rad Laboratories) and SsoAdvanced™ Universal SYBR® Green Supermix (Bio-Rad Laboratories).

The sequences of the primers used in this study were shown as follows:

(1) SCD1: (5′-TTCAGAAACACATGCTGATCCTCATAATTCCC-3′ and 5′-ATTAAGCACCACAGCATATCGCAAGAAAGTGG-3′), *PROM1* (CD133): (5′-CTGGGGCTGCTGTTTATTATTCTG-3′ and 5′-ACGCCTTGTCCTTGGTAGTGTTG-3′);
(2) CD24: (5′-TCCAAGGCACCCAGCATCCTGCTAGA-3′ and 5′-TAGAAGACGTTTCTTGGCCTGAGTCT-3′);
(3) ALDH1A1: (5′-CGGGAAAAGCAATCTGAAGAGGG-3′ and 5′-GATGCGGCTATACAACACTGGC-3′);
(4) ACTB (β-Actin): (5′-CGTCACCAACTGGGACGACA-3′ and 5′-CTTCTCGCGGTTGGCCTTGG-3′).

The relative expression of each gene was calculated through the ΔΔCT method in CFX Manager software (Bio-Rad Laboratories), and the target gene expression was normalized by the endogenous housekeeping gene ACTB β-actin. In addition, No-RT controls and No-template controls were used to avoid potential genomic DNA/RNA contaminants or other technical contaminants.

3. Results

3.1. Iri-resistant cells have higher abundances of unsaturated lipids and fatty acids than their parental cells

The drug resistance levels of control (parent HCT-116) and Iri-resistant (3-, 10-, and 20-day resistance) cells in each group were compared according to their IC_{50} (at 72 h) values, which were determined by MTT viability assay. As shown in Fig. 2A, the parental cells ($IC_{50} = 3.0 \pm 1.1$ μM) are more sensitive to Iri treatment compared to the Iri-resistant cells ($IC_{50} = 5.3 \pm 1.6$, 7.8 ± 1.2, and 11.0 ± 1.1 μM for 3-, 10-, and 20-day resistant cells, respectively). Previous studies indicate that cell lines displaying two to eight folds of increased resistance than their parental cell lines are considered as clinically relevant drug-resistant cells [65]. Therefore, our experimental results indicated that 10 and 20 days of Iri treatment produced Iri-resistant cells.

In this study, we aim to investigate the metabolomic characteristics of Iri-resistant cells as well as the mechanisms of how cancer cells establish drug resistance at the early-stage. 10- and 20-day resistance cells were used as models to study the initial drug resistance mechanisms. We first conducted SCMS experiments of the parental and 10-day Iri-resistance cells to compare their metabolic profiles. Representative mass spectra of single control and 10-day resistant cells are show in Fig. S1, and the PCA of the SCMS data from these two groups are illustrated in Fig. S2. In addition, the volcano plot is provided as Fig. S3. Using the accurate mass to search against the online databases, we were able to tentatively label 62 ions with significantly different abundances ($p < 0.05$, from *t*-test). We characterized their structures by performing MS/MS at the single-cell level combined with HPLC-MS/MS analyses of cell lysates. We were able to identify 11 and 22

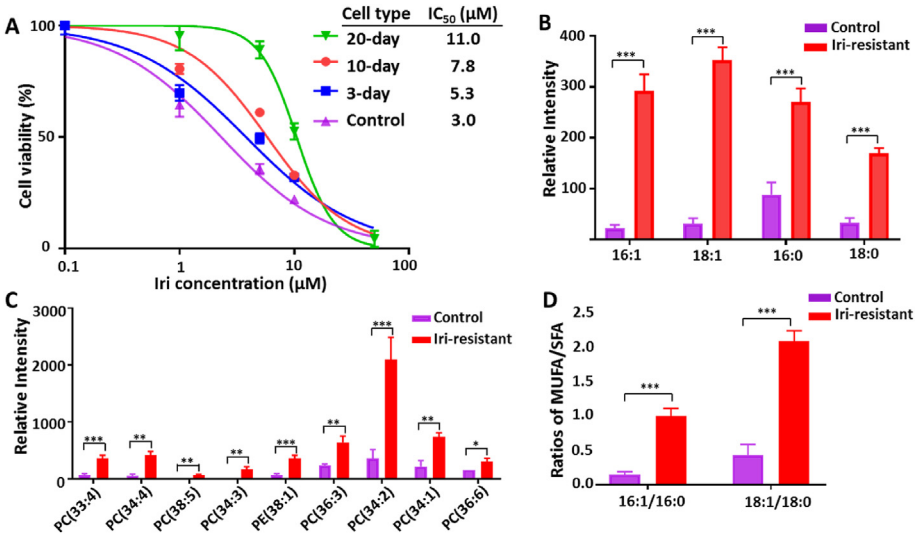

Fig. 2. Comparison of drug resistance levels and SCMS lipidomic characteristics of parental and 10-day resistant HCT-116 cells (n = 60 cells in each group in SCMS experiments). (A) Measurements of the IC_{50} of Iri (at 72 h) for the parental (control) and Iri-resistant HCT-116 cells with 3-, 10-, and 20-day resistance. IC_{50} values are represented as mean ± standard deviation (n = 5 biological replicates). (B) Relative abundances of fatty acids (C16:0, C16:1, C18:0, and C18:1) in the control and 10-day resistant cells. (C) Relative abundances of PCs (phosphatidylcholines) and PE (phosphatidylethonalamine) in the control and 10-day resistant cells. (D) Ratios of unsaturated fatty acid (UFA) to saturated fatty acid (SFA) in the control and 10-day resistant cells. (From *t*-test: *, $p < 0.05$; **, $p < 0.01$; ***, $p < 0.001$.)

ions from single cells (Fig. S4) and cell lysates (Fig. S5), respectively.

We further compared results from the SCMS and HPLC-MS/MS experiments using 10-day Iri-resistant cells (Fig. S7). Overall, more species (including identified and tentatively labeled metabolites) were observed from the LC-MS scan (1,499) than SCMS (282), most likely because cell lysate (prepared from 1 × 10 [6] cells) contains significantly larger amounts of analytes than individual cells. In addition, LC offers chromatographic separation prior to MS ionization with minimized matrix effect. However, it is worth noting that 179 unique species can only be detected in SCMS analysis. This likely indicates that these species are fragile or have rapid turnover rate in live cells, and they are potentially lost during the preparation of cell lysate [66]. Similar trend was observed in our previous studies [54].

Our results indicate that a series of cellular lipids were upregulated in Iri-resistant cells. Particularly, 10-day resistant cells have significantly higher levels of unsaturated phosphatidylcholines (PCs), including PC(33:4), PC(34:4), PC(38:5), PC(34:3), PC(36:3), PC(34:2), PC(34:1), and PC(36:6) (Fig. 2B). Moreover, four major fatty acids (C18:0 (stearic acid), C18:1 (oleic acid), C16:0 (palmitic acid), and C16:1 (palmitoleic acid)) were more abundant in 10-day resistant cells compared to the parental cells (Fig. 2C). In addition, the ratios of monounsaturated fatty acids (MUFAs) to saturated fatty acids (SFAs), such as palmitic acid/palmitoleic acid (C16:0/C16:1) and stearic acid/oleic acid (C18:0/C18:1), were dramatically increased in Iri-resistant cells (Fig. 2D). Taken together, the SCMS metabolomics results suggest that Iri-resistant cells contain significantly higher levels of unsaturated lipids and fatty acids than the parental cells.

3.2. Higher levels of lipids/fatty acids in Iri-resistant cells are mediated by SCD1

SCD1, one of the most important desaturases catalyzing SFAs to MUFAs, is regarded as a new target for studies of tumorigenesis and cancer therapy [67,68]. SCD1 is upregulated in multiple cancers, and its overexpression is associated with clinical drug resistance [67,69]. Suppressing the activities of SCD1 using the inhibits (e.g., A939572, MF-438, and CAY10566) greatly reduce cancer cell proliferation, migration, and invasion [67,68]. Because the major products from SCD1 are oleic acid (C18:1) and palmitoleic acid (C16:1) [70], upregulating SCD1 results in increased levels of unsaturated lipids and fatty acids [71]. Therefore, we hypothesize that SCD1 induced the enrichment of unsaturated lipids and fatty acids in 10-day resistant cells, and suppressing SCD1 can reduce the production of unsaturated lipids and fatty acids in Iri-resistant cells. To test this hypothesis, we conducted qPCR and western blotting experiments. Our results indicate that both SCD1 and its mRNA are significantly upregulated in 10-day resistant cells compared with the parental cells (Fig. 3A and B). We then treated 10-day resistant cells with CAY10566, a specific inhibitor of SCD1 [72], to further study the function of SCD1. Our SCMS results show that inhibiting SCD1 dramatically suppressed the turnover of SFAs to MUFAs, and therefore, significantly reduced the ratios of MUFA to SFA (C16:1/C16:0 and C18:1/C18:0) (Fig. 3C) and levels of multiple unsaturated lipids (Fig. 3D) in 10-day resistant cells. The abundance changes of these fatty acids are illustrated in Fig. 3E. Due to the inhibition of SCD1 in 10-day resistant cells, the production of C16:1 and C18:1 was greatly reduced, whereas C16:0 and C18:0 were accumulated (Fig. 3E), leading to decreased C16:1/C16:0 and C18:1/C18:0 after CAY10566 treatment (Fig. 3C).

In general, the abundances of unsaturated lipids in 10-day resistant cells were decreased upon CAY10566 treatment. Changes in lipid saturation affect cell membrane fluidity, topology, and mobility [73,74]. Particularly, increased degrees of unsaturation can make cell membrane less fluid and reduce drug-lipids interaction in cancer cells [75–77]. Similarly, relevant studies indicate that cancer stem cells also possess higher levels of unsaturated lipids and fatty acids [39,78,79]. It is interesting to note that PC(38:5) exhibited an opposite trend. Similar trends were reported in our previous studies of cancer stem cells treated by CAY10566 [39]. Although the exact mechanisms are unclear, it is likely that the accumulation of saturated fatty acids (C16:0 and C18:0), which can be used as the materials to synthesize unsaturated lipids, increased the production of PC(38:5), such as PC(16:0/22:5) and PC(18:0/20:5), through competitive pathways. In conclusion, our results indicate that the upregulation of unsaturated lipids and fatty acids are correlated to the over-expressed SCD1 in Iri-resistant cells.

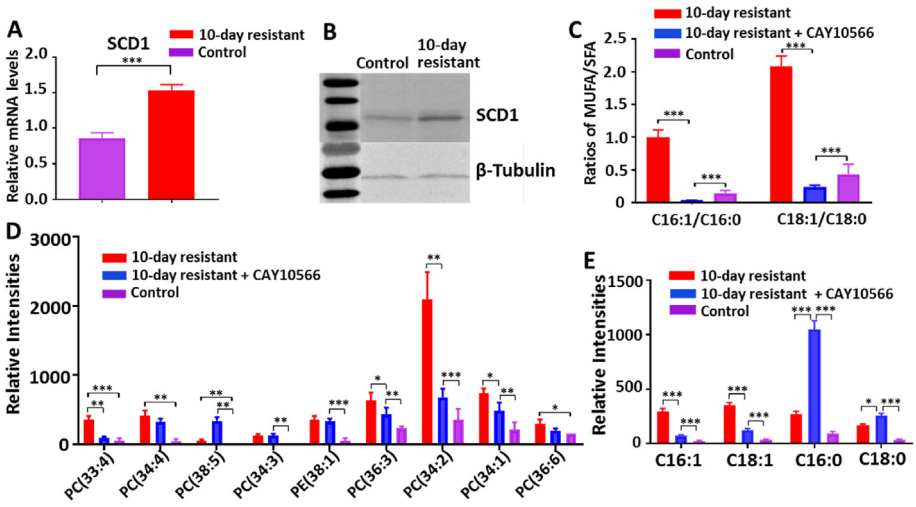

Fig. 3. Correlations between SCD1 and unsaturated fatty acids and lipids in control and 10-day resistant cells. (A) qPCR measurements of SCD1 mRNA. Relative mRNA levels were represented as mean ± standard deviation (n = 3 analytical replicates). (B) Western blot measurements of SCD1 expression. The influence of SCD1 inhibitor (CAY10566) on (C) MUFA/SFA, (D) abundances of unsaturated lipids, and (E) abundances of fatty acids. n = 60 cells in each group in SCMS experiments. (From *t*-test: *, $p < 0.05$; **, $p < 0.01$; ***, $p < 0.001$.)

3.3. SCD1 modulates drug resistance in Iri-resistant cells

In order to investigate whether SCD1 plays a role in the development of Iri resistance of cancer cells, we measured drug resistance levels of Iri-resistant cells with suppressed SCD1 activities at different degrees.

First, we studied the development of Iri resistance of cells with and without the presence of CAY10566. We incubated the parental HCT116 cells in the culture media containing Iri (1.0 μM) and CAY10566 (1.0 μM) for 10 days, and this cell line is denoted as 10-day-Iri-CAY. We then collected 10-day-Iri-CAY cells to measure their IC_{50} of Iri (at 72 h). It is worth noting that all IC_{50} measurements were performed without the presence of CAY10566, ensuring the same measurement conditions across all cell lines. Compared with the IC_{50} (7.8 ± 1.2 μM) of the 10-day resistant cells, which were produced by incubating the parental HCT116 cells in medium containing Iri (1.0 μM) for 10 days, the 10-day-Iri-CAY cells exhibited significantly reduced Iri-resistance level (IC_{50} = 4.5 ± 2.1 μM) (Fig. 4A).

Second, we alleviated the suppression of SCD1 activities in 10-day-Iri-CAY cells and then conducted cell viability measurements. 10-day-Iri-CAY cells were subjected to cell viability measurements (at 72 h) using culture media containing Iri (5.0 μM), CAY10566 (1.0 μM), and oleic acid (OA) at a series of different concentrations (i.e., 3.0, 30, and 300 μM). A moderate concentration (5.0 μM) of Iri was selected to ensure adequate numbers of cells for reliable cell viability measurements under all treatment conditions. It is worth noting that the concentration of CAY10566 (1.0 μM) was unchanged during the culture and viability measurement of 10-day-Iri-CAY cells, ensuring its continuous influence on SCD1 activities. Because OA is a major product of SCD1, inhibiting the activity of SCD1 can reduce the production of OA, whereas supplying exogenous OA during cell culture will mitigate the inhibition effects of SCD1 [39,80–82]. In fact, our experimental results show that adding exogenous OA to 10-day-Iri-CAY cells alleviated SCD1 suppression by CAY10566, and significantly increased cell viability (Fig. 4B). Taken together, we conclude SCD1 activities can modulate the resistance levels of Iri-resistant cells.

3.4. Similar molecular characteristics between the Iri-resistant cells and CSCs

It has been demonstrated that cancer therapy (e.g., radiochemotherapy and chemotherapy) could directly transform the non-stem cancer cells (NSCCs) into CSCs through the reprogramming or dedifferentiation processes trigged by ionizing radiation and chemotoxicity [17,83,84]. For example, studies found that non-stem breast cancer cells spontaneously dedifferentiated into CSCs

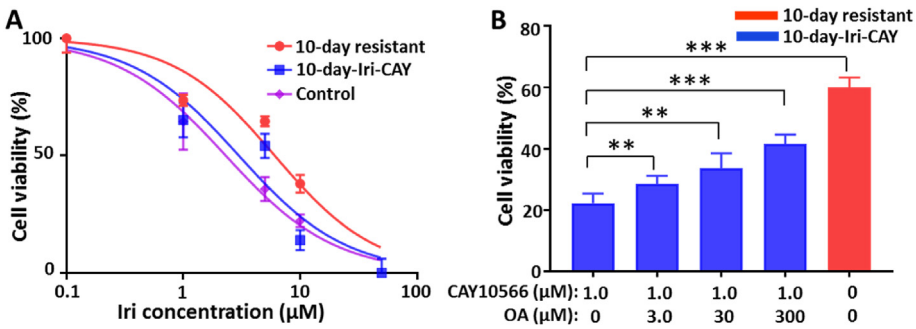

Fig. 4. The influence of SCD1 activities on the viability of Iri-resistant cells. (A) Comparison of the IC_{50} of 10-day resistant (7.8 ± 1.2 μM), 10-day-Iri-CAY (4.5 ± 2.1 μM), and control (3.0 ± 1.1 μM) cells. (B) Exogenous OA (oleic acid) alleviated the suppression effect of CAY-10566 in 10-day-Iri-CAY cells and significantly increased their viability under the treatment of Iri (5.0 μM, for 72 h). Viability of 10-day resistant cells under the same treatment of Iri (5.0 μM, for 72 h) is shown for comparison. Cell viabilities (including IC_{50} values) are represented as mean ± standard deviation (n = 5 biological replicates). (From *t*-test: *, $p < 0.05$; **, $p < 0.01$; ***, $p < 0.001$.)

in vitro and *in vivo*, whereas the mechanism of dedifferentiation process remains unclear [85]. In addition, recent studies suggested that CSCs and non-CSCs exhibit plasticity, allowing for cell state transition between them [86–88]. In the current studies, we discovered a number of molecular features of Iri-resistant cells are similar to those of CSCs. First, the SCMS results indicate that 10-day resistant cells contain higher levels of unsaturated fatty acids and lipids compared with the parental cells (Fig. 2B-D). Similar trends have been reported in the studies of colon CSCs and NSCCs [71,89]. Second, qPCR experiments demonstrate that the mRNA levels of three colon CSCs biomarkers (i.e., CD133, CD24, and ALDH1A1) are significantly increased in the 10-day resistant cells compared to the parental cells (Fig. 5A). In addition, the overexpressed CD133 and CD24 proteins in 10-day and 20-day resistant cells were confirmed by flow cytometry assay (Fig. 5B-D). Therefore, these results indicate that Iri-resistant cells possess multiple molecular characteristics similar to those of CSCs. Nevertheless, we cannot simply regard the Iri-resistant cells as CSCs without demonstrating other key properties such as self-renewal and multilineage differentiation potential [90,91]. However, these studies are beyond the scope of the current work.

3.5. SCD1 regulates the expression of CSC biomarker ALDH1A1

Given that SCD1 is essential for the maintenance of stemness in CSCs [71], we investigated the correlation between the levels of SCD1 and the expression of CSC protein biomarkers in Iri-resistant cells. We conducted qPCR measurements of the mRNA levels of CSCs biomarkers in 10-day resistant cells with and without the treatment of CAY10566 (1.0 μM, for 72 h), a SCD1 inhibitor. Our results indicate that inhibiting SCD1 had no significant influence on the expression of CD24 and CD133 (Fig. S6), but significantly reduced the mRNA level of ALDH1A1 (Fig. 6A). Moreover, adding OA (the major product of SCD1) along with CAY10566 in the treatment of 10-day Iri-resistant cells successfully rescued the mRNA level of ALDH1A1 (Fig. 6A). These results suggest that SCD1 specifically upregulates the expression of ALDH1A1, which potentially promotes the stemness development of Iri-resistance in cancer cells.

3.6. ALDH1A1 is associated with the reactive oxygen species (ROS) level in Iri-resistant cells

The function of ALDH1A1 is to catalyze oxidation of aldehydes, and the products, acetates, further contribute to cellular detoxification, retinoic acid metabolism, and protecting cell damage from reactive oxygen species (ROS) [92,93]. Compared with healthy cells, cancer cells generally possess relatively higher levels of ROS, promoting cancer development and progression. However, excessively increased amounts of ROS can induce oxidative stress in cancer cells and result in cycle arrest, cellular senescence, and apoptosis [94,95]. For example, multiple anticancer drugs (e.g., Iri, piperlongumine, mitomycin C, doxorubicin, paclitaxel, and vinblastine) can lead to an enrichment of ROS and induce cell apoptosis [96–98].

We investigated the influence of ALDH1A1 activities on the ROS levels in Iri-resistant cells. We used DEAB (N, N-diethylaminobenzaldehyde), an inhibitor of ALDH1A1 [99], to treat 10-day resistant cells, and observed significantly increased ROS levels (Fig. 6B). In contrast, combining retinoic acid (RA), which is a major product of ALDHIA1, with DEAB to treat 10-day resistant cells drastically decreased their ROS levels. We then investigated the correlation between SCD1 activities and ROS levels in 10-day resistant cells. We discovered that inhibiting SCD1 (using CAY10566) increased the ROS level, whereas adding OA (oleic acid; a major product of SCD1) rescued the inhibition effect (Fig. 6B). Our results likely indicate that Iri-resistant cells contain overexpressed SCD1 (Fig. 3B), which further results in upregulated ALDH1A1 (Figs. 5A and 6A), increased stemness, and decreased ROS level (Fig. 6B), and eventually enhance their drug resistance levels (Figs. 2A and 4A). Both levels of mRNA and ROS were measured 72 h after the individual or combinational treatment of CAY10566

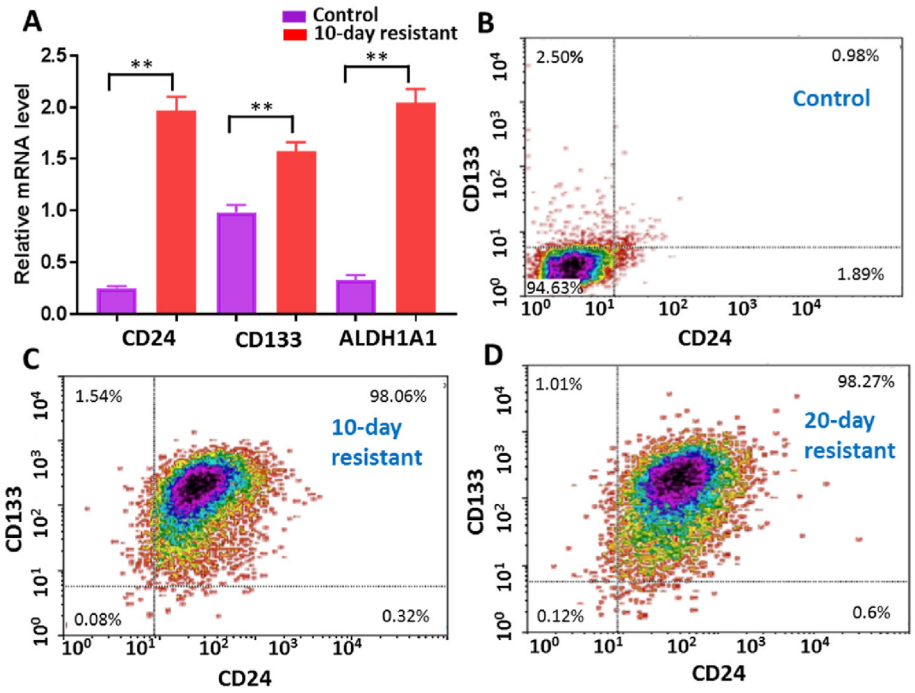

Fig. 5. Iri-resistant cells possess certain molecular characteristics of CSCs. (A) qPCR measurements of mRNA levels of CD24, CD133, and ALDH1A1 in 10-day resistant cells. Relative mRNA levels were represented as mean ± standard deviation (n = 3 analytical replicates). Flow cytometry measurements of CSC surface biomarkers CD24 and CD133 in (B) control, (C) 10-day, and (D) 20-day resistant cells. (From *t*-test: *, $p < 0.05$; **, $p < 0.01$; ***, $p < 0.001$.)

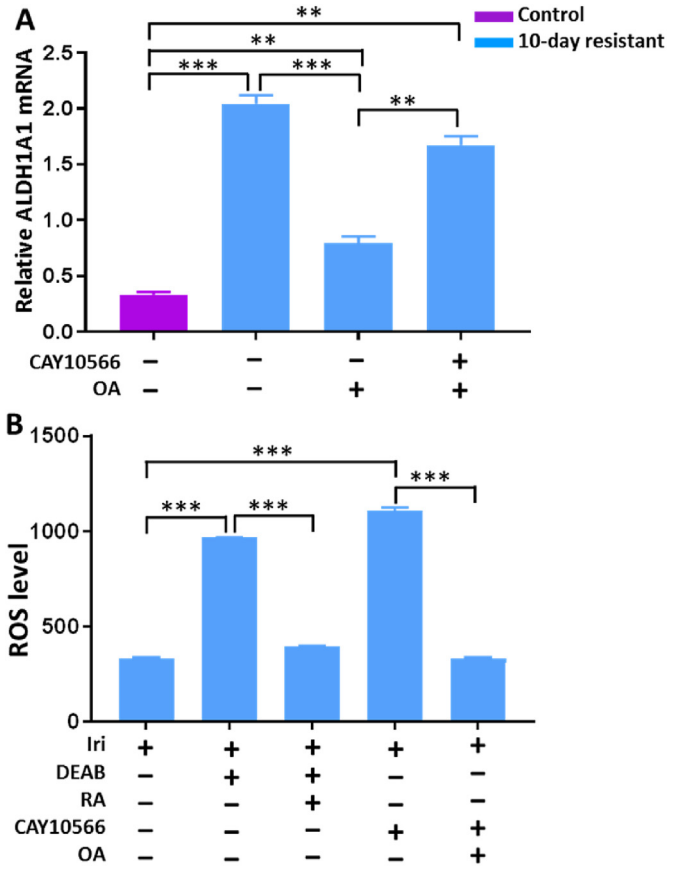

Fig. 6. Influence of SCD1 activities on ALDH1A1 expression and ROS level in 10-day resistant cells under different treatment conditions. (A) Levels of ALDH1A1 mRNA significantly affected by the treatment of SCD1 inhibitor (CAY10566) and SCD1 major product OA (oleic acid). (B) ROS levels affected by the treatment of ALDH1A1 inhibitor (DEAB), ALDH1A1 major product RA (retinoic acid), SCD1 inhibitor (CAY10566), and SCD1 major product OA. Data from both types of experiments were represented as mean ± standard deviation (n = 3 analytical replicates). (From *t*-test: *, $p < 0.05$; **, $p < 0.01$; ***, $p < 0.001$.)

(1.0 μM), OA (50 μM), DEBA (10 μM), and RA (1.0 μM). In addition, all treatments were conducted with the presence of Iri (1.0 μM) to continuously maintain its influence on Iri-resistant cells.

4. Discussion

The potency of Iri in clinical treatment is frequently diminished by *de novo* and acquired clinical resistance [100,101], whereas the chemoresistance mechanisms are generally associated with metabolic reprogramming [102–105]. For example, to escape from chemotoxicity, cancer cells may require larger supplies of metabolites to activate their defense mechanisms through enhancing glycolysis and lipogenesis [102,106]. It has been reported lipid droplets are accumulated in cancer cells upon anticancer drug treatment [107], and *de novo* lipids synthesis enzymes were enriched in the Iri-resistant cells [108]. However, it is still unknown how lipogenesis contributes to Iri-resistance.

The current study revealed a novel Iri-resistance mechanism in cell lines, in which Iri treatment activates lipid desaturase SCD1 and further results in an accumulation of unsaturated lipids and fatty acids. SCD1 is one of the major lipid desaturases catalyzing the conversion of SFAs (e.g., stearic acid (C18:0) and palmitic acid (C16:0)) to MUFAs (e.g., oleic acid (C18:1) and palmitoleic acid (C16:1)) in mammalian cells. In addition, SCD1 stimulates the conversion of FAs into other molecules (e.g., triglycerides, phospholipids, and cholesterol ester) contributing to cell membrane synthesis during cell mitosis. SCD1 has recently become a novel molecular target for cancer chemotherapy. Previous studies indicate that overexpressed SCD1 facilitated tumor survival in liver, lung, and pancreatic cancers. Inhibiting SCD1 suppressed growth and proliferation of cancer cells [109–111], and importantly, reduced drug-resistance of CSCs in different types of cancers such as lung, hepatocellular carcinomas, and ovarian cancers [112]. These studies implied the importance of SCD1 in chemoresistance. However, little is known about the role of SCD1 in Iri-resistant cells.

In our studies, we used HCT-116 colon cancer cell line and its derived Iri-resistant cells as the model systems. Compared with the parental cells, Iri-resistant cells possess several characteristics similar to those of CSCs, including higher drug-resistance, overexpressed CSC biomarkers (CD133, CD24, and ALDH1A1) [113], upregulated unsaturated lipids and fatty acids, and reduced ROS levels. CSCs are rare subsets of cancer cells with the ability to self-renew, initiate tumors, and resist anticancer treatment [114]. In general, CSCs confer the resistance to traditional therapeutic methods through multiple ways, including entering a protective quiescent state, up-regulating the expression of ATP-binding cassette (ABC) transporters, and decreasing ROS level [115]. Recent studies indicate that ionizing radiotherapy can transforming NSCCs into CSCs through up-regulated signaling pathways (e.g., Notch and Wnt) [17]. Because SCD1 is an important intermediate in Wnt protein biogenesis [116], it is suggested as a key factor affecting cancer stemness and tumor initiation capacity in ovarian and colon CSCs [71,117]. In addition, the ratios of palmitic acid/palmitoleic acid (C16:0/C16:1) and stearic acid/oleic acid (C18:0/C18:1) have positive correlations to the expression and activity of SCD1 [118]. We observed the upregulation of unsaturated lipids and fatty acids along with overexpressed SCD1 in Iri-resistant cells, suggesting that SCD1 can likely contribute to the development of cancer stemness in these cells. These featured unsaturated lipids and fatty acids can be potentially used as grouped biomarkers for the determination of Iri-resistant cells among heterogeneous cell populations.

In general, SCD1 regulates the expression of ALDH1A1 rather than other CSCs biomarkers [71,119]. This is supported by the current study: inhibiting SCD1 has no significant influence on the expression of CD133 and CD24, but drastically decreases the level of ALDH1A1 mRNA. ALDH1A1 is a well-known CSCs biomarker [120,121], and its major function is to oxidize retinal to retinoic acid (RA). This oxidation product contributes to cellular detoxification, RA metabolism, and mitigation of damage from ROS in CSCs [122]. Previous studies indicate that ROS are metabolomic byproducts of aerobic respiration, and they play essential roles in maintaining redox homeostasis. Excessively increased levels of ROS in cancer cells induce oxidative stress and DNA damage, and eventually lead to cell death [123]. Our experimental results indicate that inhibiting ALDH1A1 and SCD1 can significantly increase the ROS level, suggesting SCD1 and ALDH1A1 can likely protect cancer cells from apoptosis by maintaining their delicate balance of ROS levels.

Our finding demonstrates that the Iri-resistant cells can upregulate the expression of SCD1 and then generate higher levels of unsaturated lipids and fatty acids, which are potential biomarkers of CSCs. In addition, SCD1 directly regulates the expression of ALDH1A1, a stem cell biomarker of colon cancer, and contributes to the generation of the CSCs. Moreover, ALDH1A1 protects cancer cells damage from excessively high ROS levels, which are induced by Iri chemotherapy, by decreasing the ROS to balanced levels to avoid apoptosis. Given the importance of SCD1 in Iri-resistant cells, combining SCD1 inhibitors and Iri can be potentially effective for colon cancer treatment. The methodology reported in the current

work can likely be extended to studies of other types of anticancer drug-resistant cells. For example, the protein biomarker (e.g., CD24, CD133, and ALDH1A1) can be used to label drug-resistant cells with the corresponding antibodies with dyes for direct SCMS studies without sorting or separation. The current studies are focused on metabolites; however, more comprehensive experiments, such as integrated transcriptomics, proteomics, and metabolomics studies, can greatly enhance our understandings of the development drug resistance and cancer stemness. Although *in vivo* studies are beyond the scope of the current work, combined with other biopsy and labeling techniques, our experimental methods can be potentially used to study drug-resistant cells from animal models and patients.

CRediT authorship contribution statement

Mei Sun: Conceptualization, Methodology, Investigation, Writing – original draft. **Xingxiu Chen:** Conceptualization, Methodology, Validation, Formal analysis, Investigation. **Zhibo Yang:** Conceptualization, Supervision, Writing – review & editing, Resources, Funding acquisition.

Declaration of competing interest

The authors declare that they have no known competing financial interests or personal relationships that could have appeared to influence the work reported in this paper.

Acknowledgment

We thank the Laboratory for Molecular Biology and Cytometry Research at OUHSC (The University of Oklahoma Health Sciences Center) for the use of the Flow Cytometry and Imaging facility. We also appreciate Dr. Kun Lu and Mr. Liang Chi (University of North Carolina at Chapel Hill) for their assistance of qPCR studies. |This research project is partially supported by grants from National Institutes of Health (R01GM116116), National Science Foundation (OCE-1634630), and Research Council of the University of Oklahoma Norman Campus.

Appendix A. Supplementary data

Supplementary data to this article can be found online at https://doi.org/10.1016/j.aca.2022.339761.

References

[1] R. Siegel, K. Miller, A. Jemal, Cancer statistics, 2018, CA: Cancer J. Clin. 68 (1) (2018) 7–30.
[2] J. Mishra, J. Drummond, S.H. Quazi, S.S. Karanki, J. Shaw, B. Chen, N. Kumar, Prospective of colon cancer treatments and scope for combinatorial approach to enhanced cancer cell apoptosis, Crit. Rev. Oncol. Hematol. 86 (3) (2013) 232–250.
[3] K. Van der Jeught, H.-C. Xu, Y.-J. Li, X.-B. Lu, G. Ji, Drug resistance and new therapies in colorectal cancer, World J. Gastroenterol. 24 (34) (2018) 3834.
[4] G. Housman, S. Byler, S. Heerboth, K. Lapinska, M. Longacre, N. Snyder, S. Sarkar, Drug resistance in cancer: an overview, Cancers 6 (3) (2014) 1769–1792.
[5] M.M. Gottesman, Mechanisms of cancer drug resistance, Annu. Rev. Med. 53 (1) (2002) 615–627.
[6] V. Lopes-Rodrigues, A. Di Luca, J. Mleczko, P. Meleady, M. Henry, M. Pesic, D. Cabrera, S. Van Liempd, R.T. Lima, R. O'Connor, Identification of the metabolic alterations associated with the multidrug resistant phenotype in cancer and their intercellular transfer mediated by extracellular vesicles, Sci. Rep. 7 (2017) 44541.
[7] M. Wartenberg, M. Richter, A. Datchev, S. Günther, N. Milosevic, M.M. Bekhite, H.R. Figulla, J.M. Aran, J. Pétriz, H. Sauer, Glycolytic pyruvate regulates P-Glycoprotein expression in multicellular tumor spheroids via modulation of the intracellular redox state, J. Cell. Biochem. 109 (2) (2010) 434–446.
[8] J. Abraham, N.N. Salama, A.K. Azab, The role of P-glycoprotein in drug resistance in multiple myeloma, Leuk. Lymphoma 56 (1) (2015) 26–33.
[9] B. Bhattacharya, M.F. Mohd Omar, R. Soong, The Warburg effect and drug resistance, Br. J. Pharmacol. 173 (6) (2016) 970–979.
[10] M. McDermott, A. Eustace, S. Busschots, L. Breen, M. Clynes, N. O'Donovan, B. Stordal, In vitro development of chemotherapy and targeted therapy drug-resistant cancer cell lines: a practical guide with case studies, Front. Oncol. 4 (2014) 40.
[11] M.V.S. Amaral, A.J.D.S. Portilho, E.L. Da Silva, L.D.O. Sales, J.H.D.S. Maués, M.E.A. De Moraes, C.A. Moreira-Nunes, Establishment of drug-resistant cell lines as a model in experimental oncology: a review, Anticancer Res. 39 (12) (2019) 6443–6455.
[12] M. McDermott, A. Eustace, S. Busschots, L. Breen, M. Clynes, N. O'Donovan, B. Stordal, In vitro development of chemotherapy and targeted therapy drug-resistant cancer cell lines: a practical guide with case studies, Front. Oncol. 4 (2014) 40.
[13] K.J. Seung, I.E. Gelmanova, G.G. Peremitin, V.T. Golubchikova, V.E. Pavlova, O.B. Sirotkina, G.V. Yanova, A.K. Strelis, The effect of initial drug resistance on treatment response and acquired drug resistance during standardized short-course chemotherapy for tuberculosis, Clin. Infect. Dis. 39 (9) (2004) 1321–1328.
[14] S. MAlDHURE, F. As, A. PlAI, Influence of initial drug resistance on response to short course chemotherapy of pulmonary tuberculosis, Lung India 15 (4) (1997) 181–185.
[15] F. Yu, H. Yao, P. Zhu, X. Zhang, Q. Pan, C. Gong, Y. Huang, X. Hu, F. Su, J. Lieberman, let-7 regulates self renewal and tumorigenicity of breast cancer cells, Cell 131 (6) (2007) 1109–1123.
[16] Y. Touil, W. Igoudjil, M. Corvaisier, A.F. Dessein, J. Vandomme, D. Monte, L. Stechly, N. Skrypek, C. Langlois, G. Grard, G. Millet, E. Leteurtre, P. Dumont, S. Truant, F.R. Pruvot, M. Hebbar, F. Fan, L.M. Ellis, P. Formstecher, I. Van Seuningen, C. Gespach, R. Polakowska, G. Huet, Colon cancer cells escape 5FU chemotherapy-induced cell death by entering stemness and quiescence associated with the c-yes/YAP Axis, Clin. Cancer Res. 20 (4) (2014) 837–846.
[17] X. Chen, R. Liao, D. Li, J. Sun, Induced cancer stem cells generated by radio-chemotherapy and their therapeutic implications, Oncotarget 8 (10) (2017) 17301.
[18] M. Nishi, H. Akutsu, A. Kudoh, H. Kimura, N. Yamamoto, A. Umezawa, S.W. Lee, A. Ryo, Induced cancer stem-like cells as a model for biological screening and discovery of agents targeting phenotypic traits of cancer stem cell, Oncotarget 5 (18) (2014) 8665.
[19] G. Biagiotti, S. Fedeli, G. Tuci, L. Luconi, G. Giambastiani, A. Brandi, F. Pisaneschi, S. Cicchi, P. Paoli, Combined therapies with nanostructured carbon materials: there is room still available at the bottom, J. Mater. Chem. B 6 (14) (2018) 2022–2035.
[20] M.-K. Kang, S.-K. Kang, Tumorigenesis of chemotherapeutic drug-resistant cancer stem-like cells in brain glioma, Stem Cell. Dev. 16 (5) (2007) 837–848.
[21] C. Muschet, G. Moller, C. Prehn, M.H. de Angelis, J. Adamski, J. Tokarz, Removing the bottlenecks of cell culture metabolomics: fast normalization procedure, correlation of metabolites to cell number, and impact of the cell harvesting method, Metabolomics 12 (10) (2016).
[22] L.W. Zhang, A. Vertes, Energy charge, redox state, and metabolite turnover in single human hepatocytes revealed by capillary microsampling mass spectrometry, Anal. Chem. 87 (20) (2015) 10397–10405.
[23] S.J. Standke, D.H. Colby, R.C. Bensen, A.W.G. Burgett, Z.B. Yang, Integrated cell manipulation platform coupled with the single-probe for mass spectrometry analysis of drugs and metabolites in single suspension cells, Jove-J Vis Exp 148 (2019).
[24] N. Pan, S.J. Standke, N.R. Kothapalli, M. Sun, R.C. Bensen, A.W.G. Burgett, Z.B. Yang, Quantification of drug molecules in live single cells using the single-probe mass spectrometry technique, Anal. Chem. 91 (14) (2019) 9018–9024.
[25] H.W. Li, X. Hua, Y.T. Long, Graphene quantum dots enhanced ToF-SIMS for single-cell imaging, Anal. Bioanal. Chem. 411 (18) (2019) 4025–4030.
[26] A.F.M. Altelaar, I. Klinkert, K. Jalink, R.P.J. de Lange, R.A.H. Adan, R.M.A. Heeren, S.R. Piersma, Gold-enhanced biomolecular surface imaging of cells and tissue by SIMS and MALDI mass spectrometry, Anal. Chem. 78 (3) (2006) 734–742.
[27] T. Masujima, Live single-cell mass spectrometry, Anal. Sci. 25 (8) (2009) 953–960.
[28] X.Y. Gong, Y.Y. Zhao, S.Q. Cai, S.J. Fu, C.D. Yang, S.C. Zhang, X.R. Zhang, Single cell analysis with probe ESI-mass spectrometry: detection of metabolites at cellular and subcellular levels, Anal. Chem. 86 (8) (2014) 3809–3816.
[29] P. Nemes, A. Vertes, Laser ablation electrospray ionization for atmospheric pressure, in vivo, and imaging mass spectrometry, Anal. Chem. 79 (21) (2007) 8098–8106.
[30] N. Pan, W. Rao, N.R. Kothapalli, R.M. Liu, A.W.G. Burgett, Z.B. Yang, The single-probe: a miniaturized multifunctional device for single cell mass spectrometry analysis, Anal. Chem. 86 (19) (2014) 9376–9380.
[31] W. Rao, N. Pan, Z. Yang, Applications of the single-probe: mass spectrometry imaging and single cell analysis under ambient conditions, JoVE : JoVE (112) (2016), e53911.
[32] R. Liu, N. Pan, Y. Zhu, Z. Yang, T-probe: an integrated microscale device for online in situ single cell analysis and metabolic profiling using mass spectrometry, Anal. Chem. 90 (18) (2018) 11078–11085.
[33] Y.L. Zhu, R.M. Liu, Z.B. Yang, Redesigning the T-probe for mass spectrometry

analysis of online lysis of non-adherent single cells, Anal. Chim. Acta 1084 (2019) 53–59.
[34] Y. Zhu, W. Wang, Z. Yang, Combining mass spectrometry with paterno-buchi reaction to determine double-bond positions in lipids at the single-cell level, Anal. Chem. 92 (16) (2020) 11380–11387.
[35] N. Pan, W. Rao, S.J. Standke, Z. Yang, Using dicationic ion-pairing compounds to enhance the single cell mass spectrometry analysis using the single-probe: a microscale sampling and ionization device, Anal. Chem. 88 (13) (2016) 6812–6819.
[36] M. Sun, Z.B. Yang, B. Wawrik, Metabolomic fingerprints of individual algal cells using the single-probe mass spectrometry technique, Front. Plant Sci. 9 (2018) 10.
[37] R.M. Liu, M. Sun, G.W. Zhang, Y.P. Lan, Z.B. Yang, Towards early monitoring of chemotherapy-induced drug resistance based on single cell metabolomics: combining single-probe mass spectrometry with machine learning, Anal. Chim. Acta 1092 (2019) 42–48.
[38] S.J. Standke, D.H. Colby, R.C. Bensen, A.W.G. Burgett, Z. Yang, Mass spectrometry measurement of single suspended cells using a combined cell manipulation system and a single-probe device, Anal. Chem. 91 (3) (2019) 1738–1742.
[39] M. Sun, Z. Yang, Metabolomic studies of live single cancer stem cells using mass spectrometry, Anal. Chem. 91 (3) (2019) 2384–2391.
[40] B.L. Roberts, Z.C. Severance, R.C. Bensen, A.T. Lei, N.R. Kothapalli, J.I. Nunez, H.Y. Ma, S. Wu, S.J. Standke, Z.B. Yang, W.J. Reddig, E.L. Blewett, A.W.G. Burgett, Transient compound treatment induces a multigenerational reduction of oxysterol-binding protein (OSBP) levels and prophylactic antiviral activity, ACS Chem. Biol. 14 (2) (2019) 276–287.
[41] M. Liu, Y. Zhang, J. Yang, X. Cui, Z. Zhou, H. Zhan, K. Ding, X. Tian, Z. Yang, K.A. Fung, B.H. Edil, R.G. Postier, M.S. Bronze, M.E. Fernandez-Zapico, M.P. Stemmler, T. Brabletz, Y.P. Li, C.W. Houchen, M. Li, ZIP4 increases expression of transcription factor ZEB1 to promote integrin α3β1 signaling and inhibit expression of the gemcitabine transporter ENT1 in pancreatic cancer cells, Gastroenterology 158 (3) (2020) 679–692 e1.
[42] R.C. Bensen, S.J. Standke, D.H. Colby, N.R. Kothapalli, A.T. Le-McClain, M.A. Patten, A. Tripathi, J.E. Heinlen, Z.B. Yang, A.W.G. Burgett, Single cell mass spectrometry quantification of anticancer drugs: proof of concept in cancer patients, Acs Pharmacol. Transl. 4 (1) (2021) 96–100.
[43] W. Rao, N. Pan, X. Tian, Z.B. Yang, High-resolution ambient MS imaging of negative ions in positive ion mode: using dicationic reagents with the single-probe, J. Am. Soc. Mass Spectrom. 27 (1) (2016) 124–134.
[44] W. Rao, N. Pan, Z. Yang, High resolution tissue imaging using the single-probe mass spectrometry under ambient conditions, J. Am. Soc. Mass Spectrom. 26 (6) (2015) 986–993.
[45] X. Tian, G. Zhang, Z. Zou, Z. Yang, Anticancer drug affects metabolomic profiles in multicellular spheroids: studies using mass spectrometry imaging combined with machine learning, Anal. Chem. 91 (9) (2019) 5802–5809.
[46] X. Tian, B.E. Xie, Z. Zou, Y. Jiao, L.E. Lin, C.L. Chen, C.C. Hsu, J.M. Peng, Z.B. Yang, Multimodal imaging of amyloid plaques: fusion of the single-probe mass spectrometry image and fluorescence microscopy image, Anal. Chem. 91 (20) (2019) 12882–12889.
[47] M. Sun, X. Tian, Z. Yang, Microscale mass spectrometry analysis of extracellular metabolites in live multicellular tumor spheroids, Anal. Chem. 89 (17) (2017) 9069–9076.
[48] T. Mosmann, Rapid colorimetric assay for cellular growth and survival: application to proliferation and cytotoxicity assays, J. Immunol. Methods 65 (1–2) (1983) 55–63.
[49] M. Sun, Z.B. Yang, B. Wawrik, Metabolomic fingerprints of individual algal cells using the single-probe mass spectrometry technique, Front. Plant Sci. 9 (2018).
[50] W. Rao, N. Pan, Z. Yang, Applications of the single-probe: mass spectrometry imaging and single cell analysis under ambient conditions, JoVE : JoVE (112) (2016).
[51] N. Pan, W. Rao, N.R. Kothapalli, R.M. Liu, A.W.G. Burgett, Z. Yang, The single-probe: a miniaturized multifunctional device for single cell mass spectrometry analysis, Anal. Chem. 86 (19) (2014) 9376–9380.
[52] W. Rao, N. Pan, Z.B. Yang, High resolution tissue imaging using the single-probe mass spectrometry under ambient conditions, J. Am. Soc. Mass Spectrom. 26 (6) (2015) 986–993.
[53] I. Lanekoff, B.S. Heath, A. Liyu, M. Thomas, J.P. Carson, J. Laskin, Automated platform for high-resolution tissue imaging using nanospray desorption electrospray ionization mass spectrometry, Anal. Chem. 84 (19) (2012) 8351–8356.
[54] R. Liu, G. Zhang, M. Sun, X. Pan, Z. Yang, Integrating a generalized data analysis workflow with the Single-probe mass spectrometry experiment for single cell metabolomics, Anal. Chim. Acta 1064 (2019) 71–79.
[55] P. Romano, A. Profumo, M. Rocco, R. Mangerini, F. Ferri, A. Facchiano, Geena 2, improved automated analysis of MALDI/TOF mass spectra, BMC Bioinf. 17 (4) (2016) 61.
[56] Z.Q. Pang, J. Chong, G.Y. Zhou, D.A.D. Morais, L. Chang, M. Barrette, C. Gauthier, P.E. Jacques, S.Z. Li, J.G. Xia, MetaboAnalyst 5.0: narrowing the gap between raw spectra and functional insights, Nucleic Acids Res. 49 (W1) (2021) W388–W396.
[57] C.A. Smith, G. O'Maille, E.J. Want, C. Qin, S.A. Trauger, T.R. Brandon, D.E. Custodio, R. Abagyan, G. Siuzdak, METLIN: a metabolite mass spectral database, Ther. Drug Monit. 27 (6) (2005) 747–751.
[58] D.S. Wishart, Y.D. Feunang, A. Marcu, A.C. Guo, K. Liang, R. Vazquez-Fresno, T. Sajed, D. Johnson, C. Li, N. Karu, Z. Sayeeda, E. Lo, N. Assempour, M. Berjanskii, S. Singhal, D. Arndt, Y. Liang, H. Badran, J. Grant, A. Serra-Cayuela, Y. Liu, R. Mandal, V. Neveu, A. Pon, C. Knox, M. Wilson, C. Manach, A. Scalbert, HMDB 4.0: the human metabolome database for 2018, Nucleic Acids Res. 46 (D1) (2018) D608–D617.
[59] M. Wang, J.J. Carver, V.V. Phelan, L.M. Sanchez, N. Garg, Y. Peng, D.D. Nguyen, J. Watrous, C.A. Kapono, T. Luzzatto-Knaan, C. Porto, A. Bouslimani, A.V. Melnik, M.J. Meehan, W.T. Liu, M. Crusemann, P.D. Boudreau, E. Esquenazi, M. Sandoval-Calderon, R.D. Kersten, L.A. Pace, R.A. Quinn, K.R. Duncan, C.C. Hsu, D.J. Floros, R.G. Gavilan, K. Kleigrewe, T. Northen, R.J. Dutton, D. Parrot, E.E. Carlson, B. Aigle, C.F. Michelsen, L. Jelsbak, C. Sohlenkamp, P. Pevzner, A. Edlund, J. McLean, J. Piel, B.T. Murphy, L. Gerwick, C.C. Liaw, Y.L. Yang, H.U. Humpf, M. Maansson, R.A. Keyzers, A.C. Sims, A.R. Johnson, A.M. Sidebottom, B.E. Sedio, A. Klitgaard, C.B. Larson, C.A.B. P, D. Torres-Mendoza, D.J. Gonzalez, D.B. Silva, L.M. Marques, D.P. Demarque, E. Pociute, E.C. O'Neill, E. Briand, E.J.N. Helfrich, E.A. Granatosky, E. Glukhov, F. Ryffel, H. Houson, H. Mohimani, J.J. Kharbush, Y. Zeng, J.A. Vorholt, K.L. Kurita, P. Charusanti, K.L. McPhail, K.F. Nielsen, L. Vuong, M. Elfeki, M.F. Traxler, N. Engene, N. Koyama, O.B. Vining, R. Baric, R.R. Silva, S.J. Mascuch, S. Tomasi, S. Jenkins, V. Macherla, T. Hoffman, V. Agarwal, P.G. Williams, J. Dai, R. Neupane, J. Gurr, A.M.C. Rodriguez, A. Lamsa, C. Zhang, K. Dorrestein, B.M. Duggan, J. Almaliti, P.M. Allard, P. Phapale, L.F. Nothias, T. Alexandrov, M. Litaudon, J.L. Wolfender, J.E. Kyle, T.O. Metz, T. Peryea, D.T. Nguyen, D. VanLeer, P. Shinn, A. Jadhav, R. Muller, K.M. Waters, W. Shi, X. Liu, L. Zhang, R. Knight, P.R. Jensen, B.O. Palsson, K. Pogliano, R.G. Linington, M. Gutierrez, N.P. Lopes, W.H. Gerwick, B.S. Moore, P.C. Dorrestein, N. Bandeira, Sharing and community curation of mass spectrometry data with global natural products social molecular networking, Nat. Biotechnol. 34 (8) (2016) 828–837.
[60] A. Millner, D.Y. Lizardo, C.E. Atilla-Gokcumen, Untargeted lipidomics highlight the depletion of deoxyceramides during therapy-induced senescence, Proteomics 20 (10) (2020).
[61] R.K. Tyagi, A. Azrad, H. Degani, Y. Salomon, Simultaneous extraction of cellular lipids and water-soluble metabolites: evaluation by NMR spectroscopy, Magn. Reson. Med. 35 (2) (1996) 194–200.
[62] M.C. Chambers, B. Maclean, R. Burke, D. Amodei, D.L. Ruderman, S. Neumann, L. Gatto, B. Fischer, B. Pratt, J. Egertson, K. Hoff, D. Kessner, N. Tasman, N. Shulman, B. Frewen, T.A. Baker, M.Y. Brusniak, C. Paulse, D. Creasy, L. Flashner, K. Kani, C. Moulding, S.L. Seymour, L.M. Nuwaysir, B. Lefebvre, F. Kuhlmann, J. Roark, P. Rainer, S. Detlev, T. Hemenway, A. Huhmer, J. Langridge, B. Connolly, T. Chadick, K. Holly, J. Eckels, E.W. Deutsch, R.L. Moritz, J.E. Katz, D.B. Agus, M. MacCoss, D.L. Tabb, P. Mallick, A cross-platform toolkit for mass spectrometry and proteomics, Nat. Biotechnol. 30 (10) (2012) 918–920.
[63] T. Pluskal, S. Castillo, A. Villar-Briones, M. Oresic, MZmine 2: modular framework for processing, visualizing, and analyzing mass spectrometry-based molecular profile data, BMC Bioinf. 11 (2010) 395.
[64] L.A. Volobоueva, J. Liu, J.H. Suh, B.N. Ames, S.S. Miller, (R)-α-lipoic acid protects retinal pigment epithelial cells from oxidative damage, Investig. Ophthalmol. Vis. Sci. 46 (11) (2005) 4302–4310.
[65] M. McDermott, A. Eustace, S. Busschots, L. Breen, M. Clynes, N. O'Donovan, B. Stordal, In vitro development of chemotherapy and targeted therapy drug-resistant cancer cell lines: a practical guide with case studies, Front. Oncol. 4 (2014) 40.
[66] R.M. Liu, G.W. Zhang, M. Sun, X.L. Pan, Z.B. Yang, Integrating a generalized data analysis workflow with the Single-probe mass spectrometry experiment for single cell metabolomics, Anal. Chim. Acta 1064 (2019) 71–79.
[67] Z. Tracz-Gaszewska, P. Dobrzyn, Stearoyl-CoA desaturase 1 as a therapeutic target for the treatment of cancer, Cancers 11 (7) (2019).
[68] N. Oatman, N. Dasgupta, P. Arora, K. Choi, M.V. Gawali, N. Gupta, S. Parameswaran, J. Salomone, J.A. Reisz, S. Lawler, F. Furnari, C. Brennan, J.Q. Wu, L. Sallans, G. Gudelsky, P. Desai, B. Gebelein, M.T. Weirauch, A. D'Alessandro, K. Komurov, B. Dasgupta, Mechanisms of stearoyl CoA desaturase inhibitor sensitivity and acquired resistance in cancer, Sci. Adv. 7 (7) (2021).
[69] S. Dai, Y. Yan, Z. Xu, S. Zeng, L. Qian, L. Huo, X. Li, L. Sun, Z. Gong, SCD1 confers temozolomide resistance to human glioma cells via the akt/GSK3beta/beta-catenin signaling Axis, Front. Pharmacol. 8 (2017) 960.
[70] A.D. Southam, F.L. Khanim, R.E. Hayden, J.K. Constantinou, K.M. Koczula, R.H. Michell, M.R. Viant, M.T. Drayson, C.M. Bunce, Drug redeployment to kill leukemia and lymphoma cells by disrupting SCD1-mediated synthesis of monounsaturated fatty acids, Cancer Res. 75 (12) (2015) 2530–2540.
[71] J. Li, S. Condello, J. Thomes-Pepin, X. Ma, Y. Xia, T.D. Hurley, D. Matei, J.-X. Cheng, Lipid desaturation is a metabolic marker and therapeutic target of ovarian cancer stem cells, Cell Stem Cell 20 (3) (2017) 303–314, e5.
[72] G. Liu, J.K. Lynch, J. Freeman, B. Liu, Z. Xin, H. Zhao, M.D. Serby, P.R. Kym, T.S. Suhar, H.T. Smith, Discovery of potent, selective, orally bioavailable stearoyl-CoA desaturase 1 inhibitors, J. Med. Chem. 50 (13) (2007) 3086–3100.
[73] C. Peetla, S. Vijayaraghavalu, V. Labhasetwar, Biophysics of cell membrane lipids in cancer drug resistance: implications for drug transport and drug delivery with nanoparticles, Adv. Drug Deliv. Rev. 65 (13–14) (2013) 1686–1698.
[74] W. Szlasa, I. Zendran, A. Zalesinska, M. Tarek, J. Kulbacka, Lipid composition

of the cancer cell membrane, J. Bioenerg. Biomembr. 52 (5) (2020) 321–342.
[75] J. Kopecka, P. Trouillas, A.C. Gasparovic, E. Gazzano, Y.G. Assaraf, C. Riganti, Phospholipids and cholesterol: inducers of cancer multidrug resistance and therapeutic targets, Drug Resist. Updates 49 (2020), 100670.
[76] E. Rysman, K. Brusselmans, K. Scheys, L. Timmermans, R. Derua, S. Munck, P.P. Van Veldhoven, D. Waltregny, V.W. Daniels, J. Machiels, F. Vanderhoydonc, K. Smans, E. Waelkens, G. Verhoeven, J.V. Swinnen, De novo lipogenesis protects cancer cells from free radicals and chemotherapeutics by promoting membrane lipid saturation, Cancer Res. 70 (20) (2010) 8117–8126.
[77] S. Choi, Y.J. Yoo, H. Kim, H. Lee, H. Chung, M.H. Nam, J.Y. Moon, H.S. Lee, S. Yoon, W.Y. Kim, Clinical and biochemical relevance of monounsaturated fatty acid metabolism targeting strategy for cancer stem cell elimination in colon cancer, Biochem. Bioph. Res. Co. 519 (1) (2019) 100–105.
[78] J.J. Li, S. Condello, J. Thomes-Pepin, X.X. Ma, Y. Xia, T.D. Hurley, D. Matei, J.X. Cheng, Lipid desaturation is a metabolic marker and therapeutic target of ovarian cancer stem cells, Cell Stem Cell 20 (3) (2017), 303-+.
[79] A. Mukherjee, H.A. Kenny, E. Lengyel, Unsaturated fatty acids maintain cancer cell stemness, Cell Stem Cell 20 (3) (2017) 291–292.
[80] C. Angelucci, A. D'Alessio, F. Iacopino, G. Proietti, A. Di Leone, R. Masetti, G. Sica, Pivotal role of human stearoyl-CoA desaturases (SCD1 and 5) in breast cancer progression: oleic acid-based effect of SCD1 on cell migration and a novel pro-cell survival role for SCD5, Oncotarget 9 (36) (2018) 24364–24380.
[81] C.A. von Roemeling, L.A. Marlow, D.C. Radisky, A. Rohl, H.E. Larsen, J. Wei, H. Sasinowska, H. Zhu, R. Drake, M. Sasinowski, H.W. Tun, J.A. Copland, Functional genomics identifies novel genes essential for clear cell renal cell carcinoma tumor cell proliferation and migration, Oncotarget 5 (14) (2014) 5320–5334.
[82] A. Noto, S. Raffa, C. De Vitis, G. Roscilli, D. Malpicci, P. Coluccia, A. Di Napoli, A. Ricci, M.R. Giovagnoli, L. Aurisicchio, M.R. Torrisi, G. Ciliberto, R. Mancini, Stearoyl-CoA desaturase-1 is a key factor for lung cancer-initiating cells, Cell Death Dis. 4 (2013).
[83] R. Jandial, D.J. Waters, M.Y. Chen, Cancer stem cells can arise from differentiated neoplastic cells, Neurosurgery 69 (2) (2011) N22.
[84] B.G. Debeb, L. Lacerda, W. Xu, R. Larson, T. Solley, R. Atkinson, E.P. Sulman, N.T. Ueno, S. Krishnamurthy, J.M. Reuben, Histone deacetylase inhibitors stimulate dedifferentiation of human breast cancer cells through WNT/β-catenin signaling, Stem Cell. 30 (11) (2012) 2366–2377.
[85] C.L. Chaffer, I. Brueckmann, C. Scheel, A.J. Kaestli, P.A. Wiggins, L.O. Rodrigues, M. Brooks, F. Reinhardt, Y. Su, K. Polyak, Normal and neoplastic nonstem cells can spontaneously convert to a stem-like state, Proc. Natl. Acad. Sci. Unit. States Am. 108 (19) (2011) 7950–7955.
[86] B.G. Debeb, L. Lacerda, W. Xu, R. Larson, T. Solley, R. Atkinson, E.P. Sulman, N.T. Ueno, S. Krishnamurthy, J.M. Reuben, T.A. Buchholz, W.A. Woodward, Histone deacetylase inhibitors stimulate dedifferentiation of human breast cancer cells through WNT/beta-Catenin signaling, Stem Cell. 30 (11) (2012) 2366–2377.
[87] D. Iliopoulos, H.A. Hirsch, G.N. Wang, K. Struhl, Inducible formation of breast cancer stem cells and their dynamic equilibrium with non-stem cancer cells via IL6 secretion, P. Natl. Acad. Sci. USA. 108 (4) (2011) 1397–1402.
[88] C.L. Chaffer, I. Brueckmann, C. Scheel, A.J. Kaestli, P.A. Wiggins, L.O. Rodrigues, M. Brooks, F. Reinhardt, Y. Su, K. Polyak, L.M. Arendt, C. Kuperwasser, B. Bierie, R.A. Weinberg, Normal and neoplastic nonstem cells can spontaneously convert to a stem-like state, P. Natl. Acad. Sci. USA. 108 (19) (2011) 7950–7955.
[89] L. Tirinato, F. Pagliari, T. Limongi, M. Marini, A. Falqui, J. Seco, P. Candeloro, C. Liberale, E. Di Fabrizio, An overview of lipid droplets in cancer and cancer stem cells, Stem Cell. Int. 2017 (2017) 1–17.
[90] A.V. Molofsky, R. Pardal, S.J. Morrison, Diverse mechanisms regulate stem cell self-renewal, Curr. Opin. Cell Biol. 16 (6) (2004) 700–707.
[91] J.D. Lathia, H.P. Liu, Overview of cancer stem cells and stemness for community oncologists, Targeted Oncol. 12 (4) (2017) 387–399.
[92] S. Singh, C. Brocker, V. Koppaka, Y. Chen, B.C. Jackson, A. Matsumoto, D.C. Thompson, V. Vasiliou, Aldehyde dehydrogenases in cellular responses to oxidative/electrophilicstress, Free Radic. Biol. Med. 56 (2013) 89–101.
[93] D.W. Clark, K. Palle, Aldehyde dehydrogenases in cancer stem cells: potential as therapeutic targets, Ann. Transl. Med. 4 (24) (2016).
[94] G.Y. Liou, P. Storz, Reactive oxygen species in cancer, Free Radic. Res. 44 (5) (2010) 479–496.
[95] I.S. Okon, M.H. Zou, Mitochondrial ROS and cancer drug resistance: implications for therapy, Pharmacol. Res. 100 (2015) 170–174.
[96] A.T. Dharmaraja, Role of reactive oxygen species (ROS) in therapeutics and drug resistance in cancer and bacteria, J. Med. Chem. 60 (8) (2017) 3221–3240.
[97] C. Yokoyama, Y. Sueyoshi, M. Ema, Y. Mori, K. Takaishi, H. Hisatomi, Induction of oxidative stress by anticancer drugs in the presence and absence of cells, Oncol. Lett. 14 (5) (2017) 6066–6070.
[98] Y.F. Huang, D.J. Zhu, X.W. Chen, Q.K. Chen, Z.T. Luo, C.C. Liu, G.X. Wang, W.J. Zhang, N.Z. Liao, Curcumin enhances the effects of irinotecan on colorectal cancer cells through the generation of reactive oxygen species and activation of the endoplasmic reticulum stress pathway, Oncotarget 8 (25) (2017) 40264–40275.
[99] C.A. Morgan, B. Parajuli, C.D. Buchman, K. Dria, T.D.N. Hurley, N-diethylaminobenzaldehyde (DEAB) as a substrate and mechanism-based inhibitor for human ALDH isoenzymes, Chem. Biol. Interact. 234 (2015) 18–28.
[100] Y. Xu, M. Villalona-Calero, Irinotecan: mechanisms of tumor resistance and novel strategies for modulating its activity, Ann. Oncol. 13 (12) (2002) 1841–1851.
[101] A. Petitprez, A. K Larsen, Irinotecan resistance is accompanied by upregulation of EGFR and Src signaling in human cancer models, Curr. Pharmaceut. Des. 19 (5) (2013) 958–964.
[102] S. Dai, Y. Yan, Z. Xu, S. Zeng, L. Qian, L. Huo, X. Li, L. Sun, Z. Gong, SCD1 Confers Temozolomide resistance to human glioma cells via the Akt/GSK3β/β-Catenin signaling axis, Front. Pharmacol. 8 (2018) 960.
[103] F. Guerra, A.A. Arbini, L. Moro, Mitochondria and cancer chemoresistance, Biochim. Biophys. Acta (BBA) - Mol. Basis Dis. 1858 (8) (2017) 686–699.
[104] F. Guerra, A.A. Arbini, L. Moro, Mitochondria and cancer chemoresistance, Biochim. Biophys. Acta 1858 (8) (2017) 686–699.
[105] X. Qian, W. Xu, J. Xu, Q. Shi, J. Li, Y. Weng, Z. Jiang, L. Feng, X. Wang, J. Zhou, Enolase 1 stimulates glycolysis to promote chemoresistance in gastric cancer, Oncotarget 8 (29) (2017) 47691.
[106] Y. Zhao, E.B. Butler, M. Tan, Targeting cellular metabolism to improve cancer therapeutics, Cell Death Dis. 4 (3) (2013) e532.
[107] A.K. Cotte, V. Aires, M. Fredon, E. Limagne, V. Derangère, M. Thibaudin, E. Humblin, A. Scagliarini, J.-P.P. de Barros, P. Hillon, Lysophosphatidylcholine acyltransferase 2-mediated lipid droplet production supports colorectal cancer chemoresistance, Nat. Commun. 9 (1) (2018) 1–16.
[108] Y. Zhou, L.R. Bollu, F. Tozzi, X. Ye, R. Bhattacharya, G. Gao, E. Dupre, L. Xia, J. Lu, F. Fan, ATP citrate lyase mediates resistance of colorectal cancer cells to SN38, Mol. Cancer Therapeut. 2013 (2013) molcanther. 0098.
[109] R.A. Igal, Roles of stearoylCoA desaturase-1 in the regulation of cancer cell growth, survival and tumorigenesis, Cancers 3 (2) (2011) 2462–2477.
[110] G. Liu, S. Feng, L. Jia, C. Wang, Y. Fu, Y. Luo, Lung fibroblasts promote metastatic colonization through upregulation of stearoyl-CoA desaturase 1 in tumor cells, Oncogene 37 (11) (2018) 1519–1533.
[111] Y.H. Gao, J.Y. Li, H.Q. Xi, J.X. Cui, K.C. Zhang, J.B. Zhang, Y.M. Zhang, W. Xu, W.Q. Liang, Z.W. Zhuang, P.P. Wang, Z. Qiao, B. Wei, L. Chen, Stearoyl-CoA-desaturase-1 regulates gastric cancer stem-like properties and promotes tumour metastasis via Hippo/YAP pathway, Br. J. Cancer 122 (12) (2020) 1837–1847.
[112] M. Yi, J. Li, S. Chen, J. Cai, Y. Ban, Q. Peng, Y. Zhou, Z. Zeng, S. Peng, X. Li, Emerging role of lipid metabolism alterations in Cancer stem cells, J. Exp. Clin. Cancer Res. 37 (1) (2018) 118.
[113] R.C. Langan, J.E. Mullinax, M.T. Raiji, T. Upham, T. Summers, A. Stojadinovic, I. Avital, Colorectal cancer biomarkers and the potential role of cancer stem cells, J. Cancer 4 (3) (2013) 241.
[114] B. Bao, A. Ahmad, A.S. Azmi, S. Ali, F.H. Sarkar, Overview of cancer stem cells (CSCs) and mechanisms of their regulation: implications for cancer therapy, Curr. Protoc. Pharmacol. 61 (1) (2013) 14.25. 1–14.25. 14.
[115] M. Prieto-Vila, R.-u. Takahashi, W. Usuba, I. Kohama, T. Ochiya, Drug resistance driven by cancer stem cells and their niche, Int. J. Mol. Sci. 18 (12) (2017) 2574.
[116] J. Rios-Esteves, M.D. Resh, Stearoyl CoA desaturase is required to produce active, lipid-modified Wnt proteins, Cell Rep. 4 (6) (2013) 1072–1081.
[117] M. Sun, Z. Yang, Metabolomic studies of live single cancer stem cells using mass spectrometry, Anal. Chem. (2018).
[118] N. Rodriguez-Perez, E. Schiavi, R. Frei, R. Ferstl, P. Wawrzyniak, S. Smolinska, M. Sokolowska, N. Sievi, M. Kohler, P. Schmid-Grendelmeier, Altered fatty acid metabolism and reduced stearoyl-coenzyme a desaturase activity in asthma, Allergy 72 (11) (2017) 1744–1752.
[119] A. Noto, S. Raffa, C. De Vitis, G. Roscilli, D. Malpicci, P. Coluccia, A. Di Napoli, A. Ricci, M. Giovagnoli, L. Aurisicchio, Stearoyl-CoA desaturase-1 is a key factor for lung cancer-initiating cells, Cell Death Dis. 4 (12) (2013) e947-e947.
[120] K. Phoenix, X. Hong, S. Tannenbaum, K. Claffey, Expression of the Cancer Stem Cell Marker ALDH1A1 in Primary Breast Cancer: A Mechanism for Chemotherapy Resistance, AACR, 2009.
[121] C. Kahlert, E. Gaitzsch, G. Steinert, C. Mogler, E. Herpel, M. Hoffmeister, L. Jansen, A. Benner, H. Brenner, J. Chang-Claude, Expression analysis of aldehyde dehydrogenase 1A1 (ALDH1A1) in colon and rectal cancer in association with prognosis and response to chemotherapy, Ann. Surg Oncol. 19 (13) (2012) 4193–4201.
[122] S. Singh, C. Brocker, V. Koppaka, Y. Chen, B.C. Jackson, A. Matsumoto, D.C. Thompson, V. Vasiliou, Aldehyde dehydrogenases in cellular responses to oxidative/electrophilicstress, Free Radic. Biol. Med. 56 (2013) 89–101.
[123] C. Yokoyama, Y. Sueyoshi, M. Ema, Y. Mori, K. Takaishi, H. Hisatomi, Induction of oxidative stress by anticancer drugs in the presence and absence of cells, Oncol. Lett. 14 (5) (2017) 6066–6070.